Antitumor effects of plasma-activated solution on a murine melanoma model *in vivo* and *in vitro*

XINGYU YANG[1*], CHENG CHEN[1*], SHIYUN ZHOU[1], MIAOMIAO REN[1], CHENCHEN ZHANG[1], CHENG CHENG[2] and CHUNJUN YANG[1]

[1]Department of Dermatology, The Second Affiliated Hospital, Anhui Medical University, Hefei, Anhui 230601, P.R. China; [2]The Institute of Plasma Physics, Chinese Academy of Science, Hefei, Anhui 230000, P.R. China

Received January 30, 2024; Accepted October 16, 2024

DOI: 10.3892/ol.2024.14821

Abstract. Melanoma is a common malignant skin tumor with highly invasive features and a high metastasis rate that can be difficult to treat clinically. Large-scale resection of primary cutaneous melanoma is often used to avoid post-operative recurrence. For advanced patients, radiotherapy, targeted therapy and immunotherapy are often needed. Low-temperature plasma has been proved to have significant antitumor effects on a variety of cancer cell lines cultured *in vitro*. The main limitation of direct low-temperature plasma treatment is that it has weak penetration ability and can only treat superficial lesions. In recent years, research on low-temperature plasma-activated solution has revealed that it also have good antitumor effects and low-temperature plasma penetration depth problems can be solved by local injection. The present study revealed that low-temperature plasma-activated phosphate buffer solution exhibited good antitumor effects and biosafety against melanoma *in vitro* and *in vivo*. It demonstrated that low-temperature plasma-activated solution has antitumor effects due to its regulation of intracellular redox, destruction of mitochondrial function and DNA damage. *In vivo* experiments demonstrated that treatment with low-temperature plasma-activated solution not only exhibited antitumor effects but also caused no significant damage to hematopoietic function or liver and kidney functions in mice. All these results demonstrated that low-temperature plasma-activated solution represent a promising antitumor treatment strategy.

Correspondence to: Professor Chunjun Yang, Department of Dermatology, The Second Affiliated Hospital, Anhui Medical University, 678 Furong Road, Shushan, Hefei, Anhui 230601, P.R. China
E-mail: yangchunjun9@163.com

*Contributed equally

Key words: cold atmospheric plasma, plasma-activated solution, melanoma, DNA damage, mitochondrial damage, intratumoral injection

Introduction

Low-temperature plasma is an ionized gas at approximately room temperature that is composed of charged particles, neutral particles and electrons (1). Over the past two decades, low-temperature plasma medicine, as a newly developed discipline, has made preliminary achievements in disinfection and sterilization, wound healing, antitumor effects and other applications (2-4). In *in vitro* experiments, low-temperature plasma inhibits proliferation and induces apoptosis in a variety of tumor cell lines (5-7), but the mechanism has not been fully clarified. *In vitro*, low-temperature plasma initially contacts the cell culture medium, resulting in a series of complex physical and chemical reactions (8). The active substances (reactive nitrogen and oxygen species) in solution further interact with cells to exert antitumor effects (1,6,8). This finding confirms that the low-temperature plasma-activated solution (PAS) also has good antitumor effects and eliminates the limitation of the shallow penetration depth of direct treatment with low-temperature plasma (9). Therefore, low-temperature PAS treatment has the advantages of eliminating the limitations of instruments and equipment and convenient storage (10,11).

The skin is the largest and most superficial organ of the human body. This characteristic gives low-temperature plasma broad application prospects in skin diseases (12). Melanoma is a malignant tumor derived from melanin. Epidemiological analysis revealed that its incidence and mortality rates have been increasing in recent decades (13). Malignant melanoma is more common in the skin but can also occur in the mucosa, respiratory tract, gastrointestinal tract, reproductive system and other parts of the skin and is characterized by early metastasis and a high recurrence rate (14,15). The incidence of melanoma is greater in light-skinned individuals. Importantly, melanoma is one of the most common malignant tumors in young individuals and the mortality rate in young individuals is greater than that of most other cancers (16,17). Surgical resection is generally used for early localized lesions, whereas comprehensive treatments, including cytotoxic drug chemotherapy, immunotherapy and molecular targeted therapy, are used for patients with late-stage disease or multiple organ metastases (14,18). However, these treatments often cannot yield satisfactory results. Therefore, more effective methods need to be developed for the adjuvant treatment of melanoma (13).

The present study used the melanoma cell line A375 as the experimental object and used low-temperature plasma-activated phosphate buffer solution (PBS) as the medium to observe the imbalance in reactive oxygen species (ROS) levels and mitochondrial and DNA damage in A375 cells treated with PAS. *In vivo*, the antitumor effect of a PAS on subcutaneously transplanted melanoma in nude mice was observed by intratumoral injection. Moreover, the biological safety of PAS was evaluated by monitoring the weight, blood parameters and liver and kidney functions of the mice.

Materials and methods

Low-temperature plasma equipment and preparation of low-temperature PAS. Low-temperature plasma equipment was provided by the Institute of Plasma Physics, Chinese Academy of Sciences. The equipment mainly consists of a high-voltage electrode, a grounding electrode and a power supply (Fig. 1A). Two electrodes were placed in the center of the PBS dish. The spacing between the liquid surface and the high-voltage electrode was fixed at 5 mm. The power supply was set to a constant voltage of 40 V and a current of 2 A. The time of PBS exposure to low-temperature plasma is defined as the dose of the PAS. The prepared PAS was used to treat cells cultured *in vitro* and subcutaneous tumors in nude mice. In the *in vivo* experiment, 50 μl of the PAS was injected intratumorally every two days. The chemotherapy drug cisplatin (QlU Pharmaceutical Co. Ltd.; batch no. aa2a0038b) was injected into the caudal vein to treat the tumors in the positive control group. The drug concentration was 5 mg/kg and the injection volume was 1 mg/ml (Fig. 1B and C).

Cell culture. A375 melanoma cell line (American Type Culture Collection) was grown in RPMI-1640 medium (cat. no. G4531; Wuhan Servicebio Technology Co., Ltd.) supplemented with 10% FBS (cat. no. C04001; Shanghai VivaCell Biosciences, Ltd.) and 1% penicillin and streptomycin (cat. no. C0222; Beyotime Institute of Biotechnology). The cells were cultured in a culture flask (cat. no. CCF-T25H; Wuhan Servicebio Technology Co., Ltd.) in a humid environment at 37˚C and 5% CO_2 and passaged every 2-3 days.

Cell viability. Cell viability was determined using MTT assay. Cells in the logarithmic growth stage were digested, counted and inoculated into 96-well cell culture plates. Each well contained 10,000 cells and 100 μl of culture medium. After 24 h of culture, the experiment was conducted once the cells had adhered completely to the surface of the wells. After the cells were treated with PAS for 1 h, fresh medium was added to the culture plate and the culture was continued for 24 h. The antioxidant catalase (cat. no. s0082; Beyotime Institute of Biotechnology) was added to each well of the control group. MTT reagent was added to the culture plate and the absorbance at 570 nm was detected using a SpectroMax i3x (Molecular Devices, LLC).

Intracellular reactive oxygen species (ROS). The ROS kit was purchased from Beyotime Institute of Biotechnology Biological Company (cat. no. s0033s). The cell inoculation procedure was consistent with that used for the MTT assay. The fluorescent probe DCFH-DA was added to the cell culture and the changes in cellular ROS levels were measured after cells were treated with PAS for 1 h. Using a SpectroMax i3x (Molecular Devices, LLC) fluorescence microplate reader, fluorescence was determined at an excitation wavelength of 488 nm and an emission wavelength of 525 nm and the level of ROS was detected.

Mitochondrial membrane potential. A JC-1 kit was used to detect the mitochondrial membrane potential (cat. no. c2006; Beyotime Institute of Biotechnology). Cells in the logarithmic growth phase were harvested and inoculated into 10-mm diameter circular cell culture dishes. When the cell density was ~70%, the cells were treated with PAS for 1 h. The cells were stained and washed with JC-1 stain followed by JC-1 buffer. The cells were observed with fluorescence microscopy. When detecting the JC-1 monomer, the excitation wavelength was set to 490 nm and the emission wavelength was set to 530 nm. When detecting the JC-1 polymer, the excitation wavelength was set to 525 nm and the emission wavelength was set to 590 nm.

DNA damage marker. Intracellular DNA damage was detected using immunofluorescence. The cells were inoculated and cultured in 10-mm cell culture dishes and the experiment was performed when the cell density reached 70%. Histone family 2A variant (H2AX) was used as a marker of DNA damage. The H2AX antibody was purchased from Abcam (cat no. ab81299) and the fluorescent secondary antibody FITC was purchased from Beyotime Institute of Biotechnology (cat no. a0562). After the cells were treated with PAS for 1 h, they were fixed with methanol at -20˚C overnight. After the cells were washed, primary antibody diluent was added and the cells were incubated overnight at 4˚C. After the cells were rinsed again, they were incubated with a FITC-conjugated secondary antibody in the dark at room temperature for 30 min. Then, the cells were observed under a fluorescence microscope.

Western blotting. For western blot analysis, cells were seeded in 6-well plates. When the cells were completely attached to the plate, they were treated with PAS and cultivated for 8 h. The cells were then washed three times with ice-cold PBS. RIPA solution (cat no. p0013B; Beyotime Institute of Biotechnology), protease inhibitor and phosphatase inhibitor (cat no. p1050; Beyotime Institute of Biotechnology) were added to the wells at a ratio of 100:1:2. After 30 min of lysis on ice, the cell lysates were scraped and collected in Eppendorf tubes. The protein concentrations were determined using a BCA Protein Assay Kit (Beyotime Institute of Biotechnology) after centrifuging the lysates at 16,363 x g at 4˚C for 25 min. Using a 7.5% gel, proteins were separated electrophoretically after loading 10 ug of protein per lane and then transferred to a PVDF membrane. Next, the PVDF membranes were blocked for 30 min with protein-free rapid blocking buffer (EpiZyme, Inc.) at 4˚C and incubated overnight at 4˚C with the corresponding primary antibodies (H2AX, 1:10,00; Cell Signaling Technology cat no. 7631T; γ-H2AX, 1:10,00; Cell Signaling Technology cat no. 2577S; GAPDH: Dilution 1:50,00; Proteintech cat no. 10494-1-AP). The membranes were incubated for 1 h at indoor temperature with the corresponding secondary

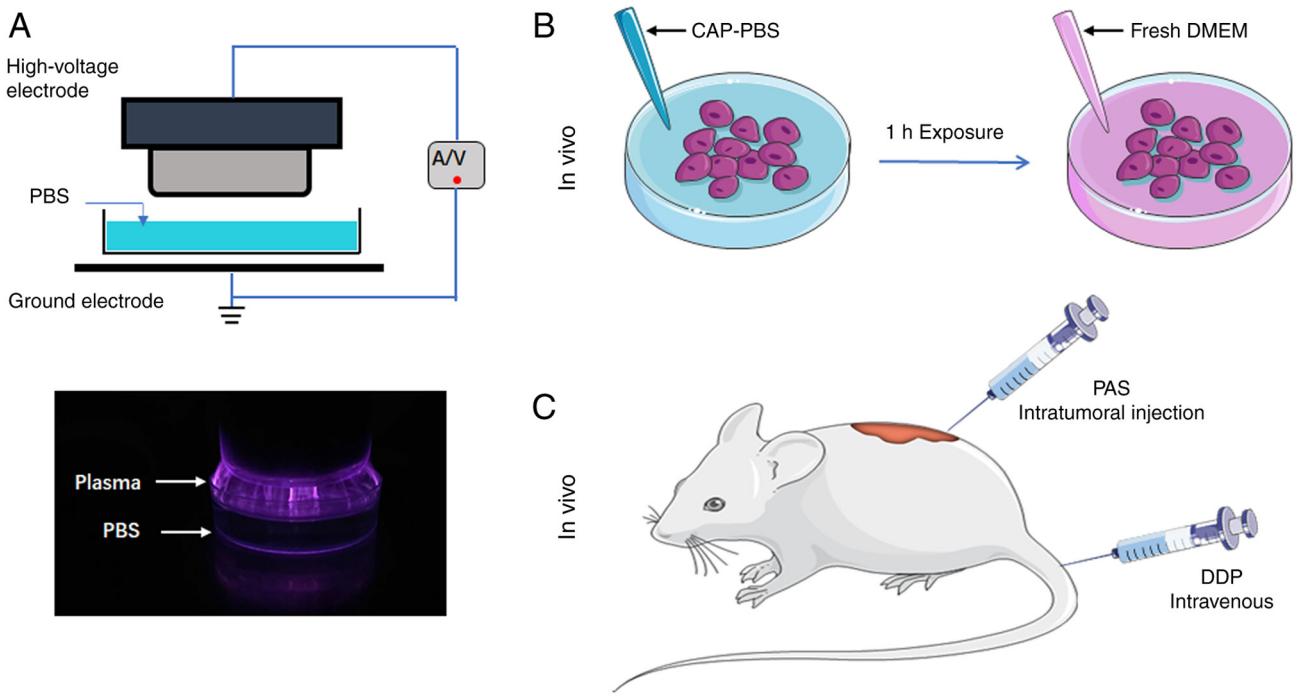

Figure 1. CAP apparatus used in the present study and the experimental schematic. (A) PBS was activated with CAP. The CAP equipment was used in the dark. (B) Cells were exposed to PAS for 1 h. (C) Intratumoral injection of PAS and tail vein injection of DDP. CAP, cold atmospheric plasma; PBS, phosphate buffer solution; PAS, plasma-activated solution; DDP, cis-dichlorodiamineplatinum.

antibodies (Dilution 1:10,000; ProteinTech cat no. SA00001-2, SA00001-1) on the next day and protein bands were visualized with visualization reagent (Biosharp; cat no. BL520A) using a western blot imaging instrument (Thermo Fisher Scientific, Inc.). Bands of interest were analyzed using ImageJ (win-java8, National Institutes of Health).

Cell subunits. Changes in intracellular subunits in A375 cells treated with PAS were observed using transmission electron microscopy. A375 cells were exposed to PAS for 1 h and then fresh medium was added to continue the cultures for 6 h for improved observation of organelle morphology. The cells were then collected by digestion and centrifugation. Glutaraldehyde (3%) was added and the cells were fixed overnight at 4˚C. Then, 1% osmium tetroxide was added to the samples and the cells were collected following a series of ethanol dehydrations. The samples were treated at room temperature with epoxy resin (Sigma Aldrich; cat no. 31185) and acetone (v/v=1/1) for 1 h, epoxy resin and acetone (V/V=3/1) for 3 h. The osmotically treated samples were embedded and heated at 70˚C overnight to obtain the embedded samples. The samples were dried and cut into 80 nm sections on an ultrathin microtome, and then stained with lead citrate solution and hydrogen peroxide acetic acid 50% ethanol saturated solution for 5 min each at room temperature and then the cell morphology was observed by transmission electron microscopy. Photographs were analyzed and processed using Digital Micrograph (Digital Micrograph 3.5, Gatan USA, Inc.).

Subcutaneous tumor transplantation in nude mice. A375 cells in logarithmic growth were inoculated subcutaneously into BALB/c-nu mice at a density of $5x10^6$ cells/100 μl/mouse. When the mean tumor volume reached ~90 mm^3, 20 mice were randomly divided into 4 groups (G1-4) of 5 mice each according to the tumor volume. Group G1 was the negative control; 50 μl PBS was injected into the tumors. In addition, 50 μl PAS was injected into the tumors in Groups G2 and G3. Group G4 mice were subjected to cisplatin tail vein injection as a positive control group. The day of grouping was defined as day 0, which was also the day of administration. The drugs were administered every 2 days for 2 weeks. After initiation of drug administration, tumor size was observed and mice were weighed on days 0, 3, 6, 9, 12 and 15. The humane endpoints identified in the present study were as follows: i) Tumor volume exceeding 3,000 mm^3 in a single mouse; ii) persistent loose stools; iii) retarded activity (unable to eat or drink); iv) arching of the back and lying on the side; v) decreased activity and signs of muscle wasting; vi) difficulty in breathing; vii) processive lowering of body temperature; viii) paralysis and/or spasms; ix) persistent bleeding; x) inability of the animal to move normally due to a tumor that is too large or for other reasons; and xi) inability to move normally due to severe ascites or increased abdominal circumference. The endpoint of the experiment was day 15 post-dose. Blood collection was performed through the submandibular vein of mice before the endpoint of the experiment, collecting 50 μl per mouse and then the samples were sent to Jiangsu GemPharmatech Co., Ltd. for the testing of blood indexes and liver and kidney functions, no anesthetic injection was administered prior to submandibular blood collection. Mice were sacrificed using cervical dislocation and the complete absence of vital signs was confirmed by observing the pinch reflex of the animals. Tumor was removed, weighed, and the tumor tissue specimen was fixed in formalin for 12 h, dehydrated, embedded in

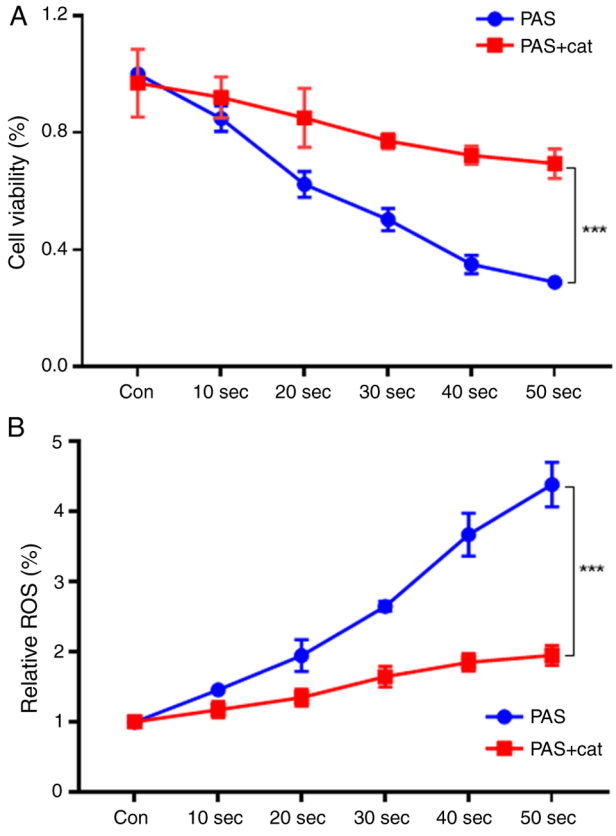

Figure 2. Cell viability and intracellular ROS detection. (A) A375 cells were exposed to PAS solution and PAS + catalase solution for 1 h and allowed to grow for an additional 24 h after the medium was changed to fresh medium. An MTT assay was utilized to detect cell viability. (B) After 1 h of PAS and PAS + catalase treatment, the cells were stained with dichloro-dihydro-fluorescein diacetate and fluorescence was measured using a microplate reader to assess changes in ROS levels in A375 cells. ***P<0.001. ROS, reactive oxygen species; PAS, plasma-activated solution.

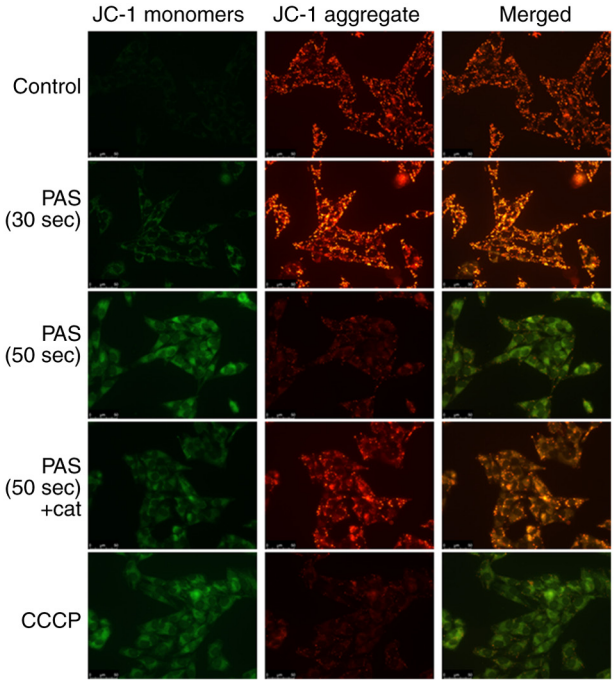

Figure 3. Detection of the mitochondrial membrane potential. A375 cells were exposed to different concentrations of PAS solution and PAS + catalase solution for 1 h. The cells were subsequently stained and washed with JC-1 staining solution and JC-1 buffer solution and changes in the mitochondrial membrane potential were observed under a fluorescence microscope. Magnification, x200x. CCCP treatment served as a positive control. PAS, plasma-activated solution; cat, catalase; CCCP, carbonyl cyanide 3-chlorophenylhydrazone.

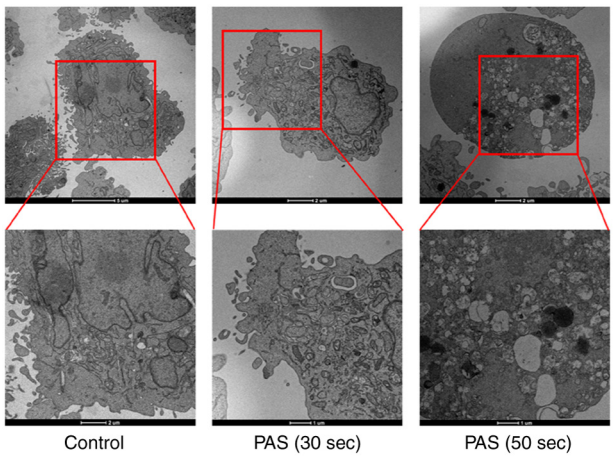

Figure 4. Transmission electron microscopy of intracellular subunits. The mitochondria exhibited a variety of sizes and shapes. Most mitochondria were visibly swollen and the mitochondria were turbid, disorganized, or cracked.

paraffin, and cut into 4-micron sections. Tissue sections were dewaxed, dehydrated and immersed in methanol containing 0.3% hydrogen peroxide for 30 min. The sections were heated in an autoclave containing 10 mM EDTA) buffer (pH 8.0) for 2 min. Sections were incubated in 1% blocking serum for 30 min to minimize non-specific binding. The sections are then incubated with primary antibody (1:250) at 4˚C overnight. Sections were then incubated with biotinylated secondary antiserum, followed by incubation with horseradish peroxidase-conjugated streptavidin-biotin complex. Finally, sections were visualized with DAB) and stained with hematoxylin. Tumor tissue sections were deparaffinized and stained with hematoxylin for 4 min at room temperature, rinsed under running water for 10 min and differentiated with ethanol hydrochloride for 3 s. Sections were again rinsed under running water until they returned blue, and then stained at room temperature with eosin for 1 min. The cellular experiments, mouse feeding, mouse modelling, blood sample collection and tumor sample collection of the present study were performed at Anhui Medical University (Anhui, China) and blood sample analysis and tumor immunohistochemistry were performed at Jiangsu GemPharmatech Co., Ltd. No mice in this experiment reached the humane endpoints. The content related to animal use and the experiments in this experimental scheme were reviewed and approved by the IACUC Committee (Anhui, China).

Statistical analysis. The results of the experiments were expressed as mean ± standard error of the mean. Comparisons between the two groups of samples were made using the independent samples paired Student's t-test, Kruskal-Wallis tests were used for datasets containing ≥3 groups and the data were

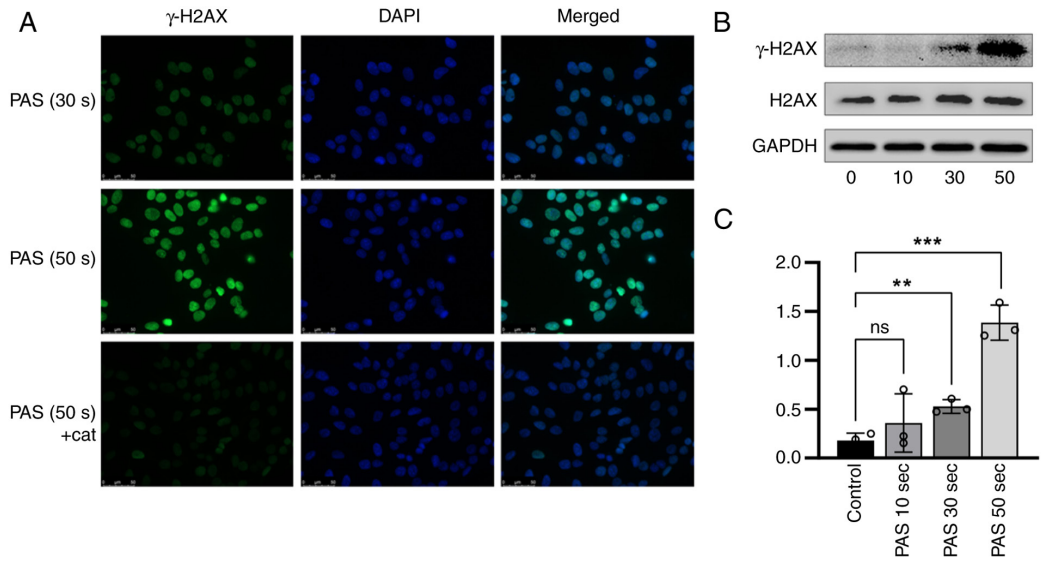

Figure 5. The DNA damage marker γ-H2AX was detected in cells using immunofluorescence and western blotting. (A) Intracellular DNA damage was detected using immunofluorescence. A375 cells were treated with PAS at different concentrations and PAS + cat for 1 h. Scale bar, 50 μm. Magnification, x200x. Nuclei were stained with DAPI (blue fluorescence). γ-H2AX was stained with Beyotime Institute of Biotechnology cat. no. a0562 (green fluorescence). (B) Western blotting analysis of γ-H2AX and H2AX in A375 cells treated with different concentrations of plasma-activated solutions. GAPDH served as the internal control. (C) γ-H2AX and H2AX expression levels were quantitatively analyzed. Each set of strips was transferred from the same film. **P<0.01, ***P<0.001, ns, not significant. H2AX, histone family 2A variant; PAS, plasma-activated solution; cat, catalase.

analyzed using SPSS (IBM SPSS Statistics 25) P<0.05 was considered to indicate a statistically significant difference.

Results

Treatment with a PAS decreases cell viability and increases intracellular ROS levels. As shown in Fig. 2A, after A375 cells were treated with different doses of the PAS for 10-50 sec, the cell viability tended to decrease. Treatment with a 50-sec dose of PAS for 1 h resulted in a cell survival rate of ~30% after 24 h. Under the same conditions, the survival rate of cells treated with the antioxidant catalase increased significantly. Intracellular ROS in the PAS group increased significantly compared with the control group. By contrast, the intracellular ROS level increased only slightly after the cells were cotreated with the antioxidant catalase (Fig. 2B).

Low-temperature plasma-activated solution treatment induces mitochondrial and DNA damage. A decrease in the mitochondrial membrane potential is a hallmark feature of apoptosis (19) JC-1 accumulates in the mitochondrial matrix and forms polymers (J-aggregates) that produce red fluorescence when the mitochondrial membrane potential is high and the JC-1 monomer produces green fluorescence when the mitochondrial membrane potential is low. As shown in Fig. 3, after the cells were subject to PAS treatment, the mitochondrial membrane potential decreased. This decreasing trend was dose dependent. The antioxidant catalase was able to effectively alleviate this effect. Carbonyl cyanide 3-chlorophenylhydrazone (CCCP) was used as a positive control of reduced mitochondrial membrane potential.

The cells subject to PAS treatment were observed using transmission electron microscopy. Dense microvilli were observed in the cell membranes of the normal control group. The nuclei were large and centered and the organelle structures were normal. After PAS treatment, the cell volume gradually decreased. Moreover, the microvilli of the cell membranes were reduced and the nuclei were smaller. Different sizes and diverse shapes of mitochondria were observed. Most mitochondria were obviously swollen and the cristae of the mitochondria were fuzzy, disordered and even broken. Vacuole formation in the cell indicated inevitable cell death (Fig. 4). A number of DNA damage markers were also detected by immunofluorescence and western blotting. γ-H2AX was overexpressed after A375 cells were treated with PAS and the degree of injury remained dose dependent (Fig. 5).

In vivo experiments confirm that plasma-activated solution can effectively exert antitumor effects. As shown in Fig. 6A, mice in each group were administered the appropriate drugs every two days and the experimental process lasted for 15 days. The G1-G3 groups received intratumoral injections and the chemotherapy drug cisplatin was administered to the G4 group through caudal vein injection. The mice in the cisplatin group experienced significant weight loss and could not eat after the 8th day, so the treatment was stopped (Fig. 6B). Fig. 6C shows the subcutaneous tumors of the mice in each group that were removed after the experiment. As shown in Fig. 6D, compared with the control group, the G2 group (TGitv=33.73%) showed a tumor growth inhibition effect, but the difference was not significant (P>0.05; Fig. 6D). The G3 group (TGitv=39.36%) showed significant tumor growth inhibition and the G4 chemotherapy drug group (cisplatin; TGitv=66.54%) also showed significant tumor growth inhibition. Following the experiment, the tumors were removed from the mice. The size of the subcutaneous tumors decreased significantly from the G1 group to the G4 group. Tumor weight measurements revealed that

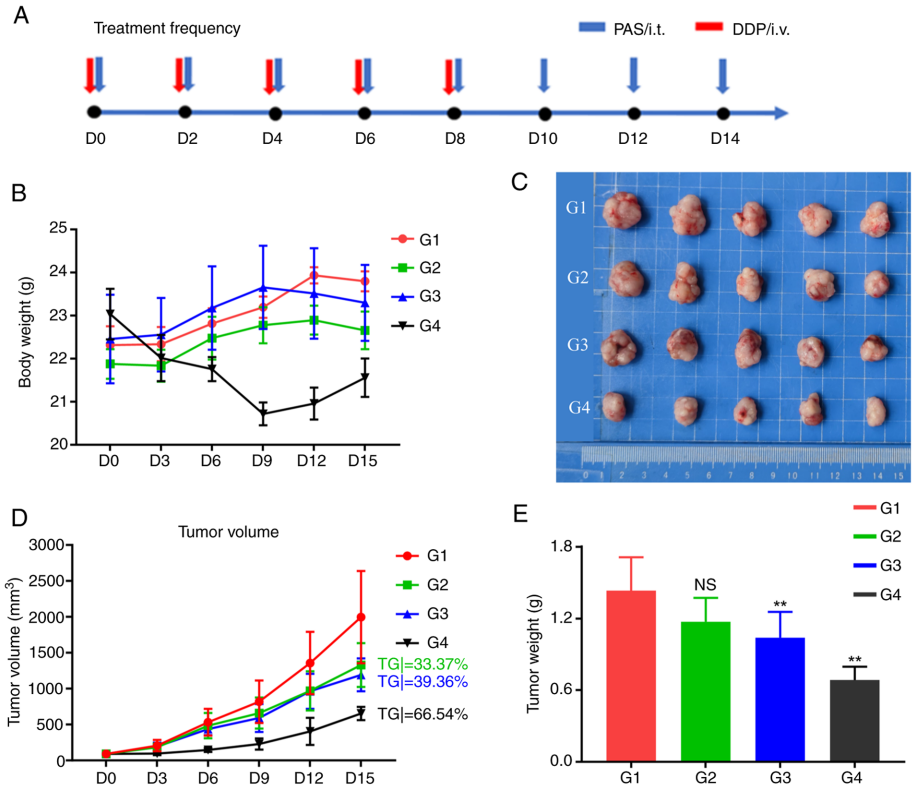

Figure 6. Tumor inhibitory effect of PAS *in vivo*. A total of 5x10^6 A375 cells/100 μl/mice were subcutaneously inoculated into BALB/nude mice. A total of 20 mice were divided into four groups (G1-4) according to tumor volume. G1 was administered an intratumor injection of PBS solution as the negative control group. G2-3 were administered an intratumor injection of PAS and G4 was administered a caudal vein injection of cisplatin as the positive control group. (A) The grouping day was defined as day 0 and the mice in each group were administered the indicated drugs every 2 days for 15 days. G4 treatment was discontinued on day 8. (B) Changes in the weights of the mice in the four groups, which were weighed every three days. (C) Tumor resection after treatment. (D) Tumor volumes were measured every three days. (E) Comparison of tumor quality among the four groups. **P<0.01. PAS, plasma-activated solution; PBS, phosphate buffer solution; DDP, cis-dichlorodiamineplatinum.

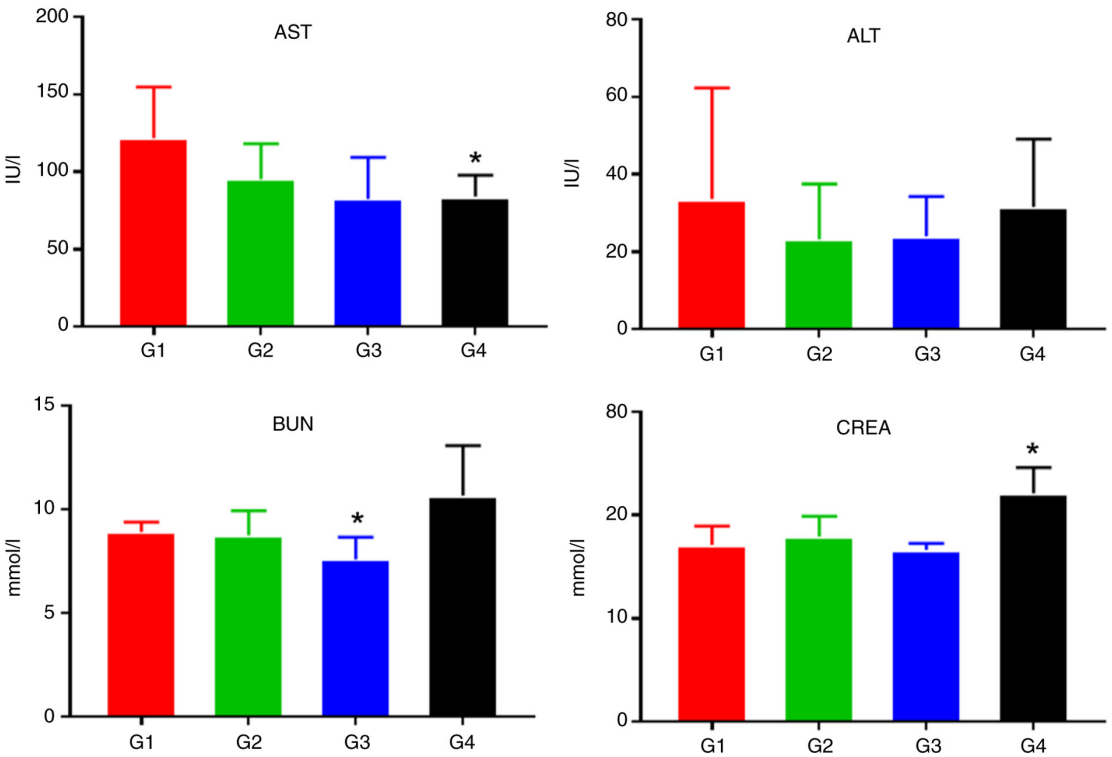

Figure 7. Hepatic/renal function analyses of PAS- and DDP-treated mice. Mouse blood samples were collected before tumor resection. *P<0.05. PAS, plasma-activated solution; DDP, cis-dichlorodiamineplatinum; AST, glutamic-oxaloacetic transaminase; ALT, glutamic-pyruvic transaminase; BUN, blood urea nitrogen; CREA, creatinine.

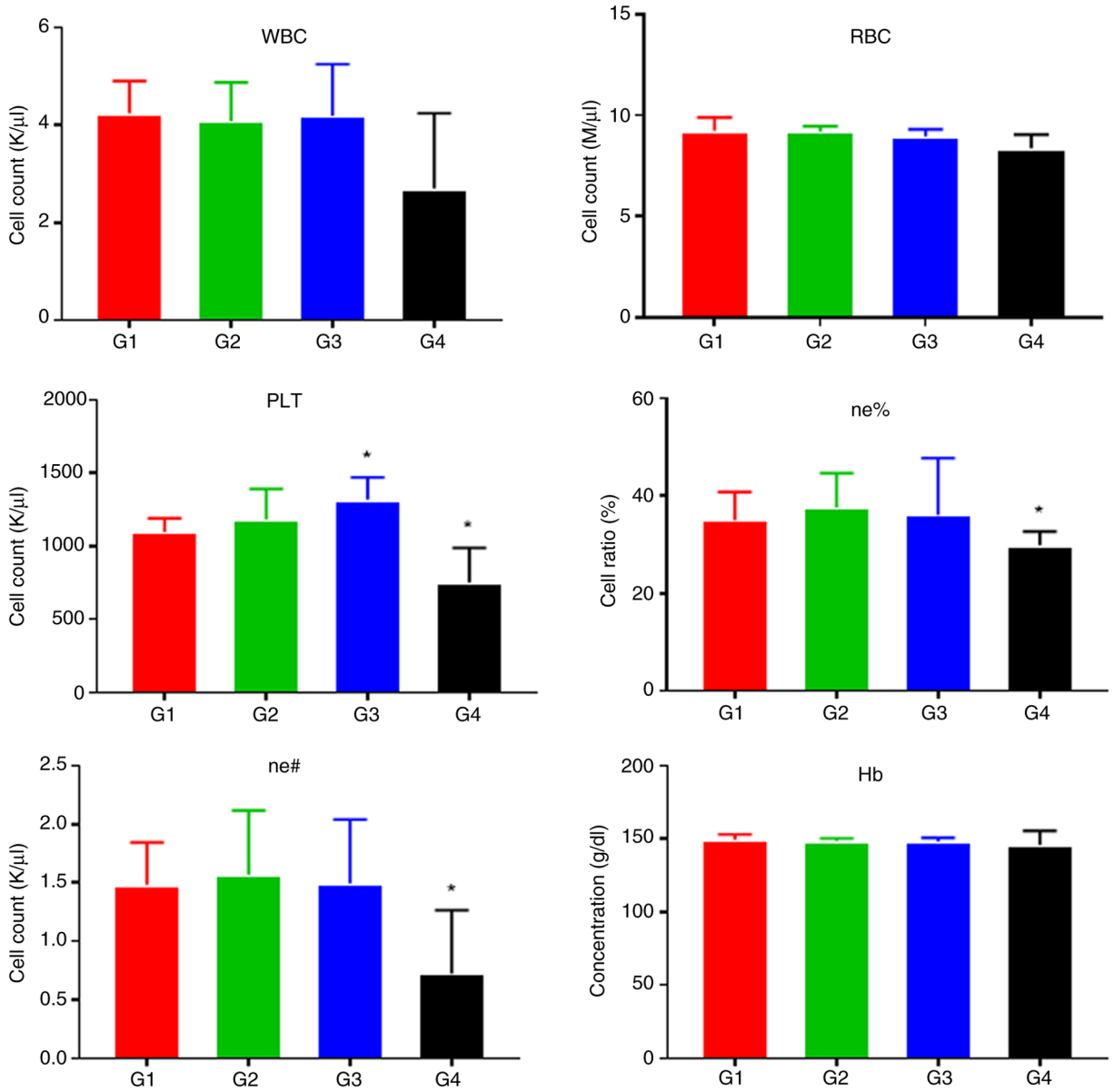

Figure 8. Routine blood tests of mice in the different groups. Blood samples were collected before tumor removal. *P<0.05. WBC, leukocytes. RBC erythrocytes. PLT, erythrocyte; ne%, neutrophil percentage; ne#, neutrophil number; Hb, hemoglobin.

tumor growth was significantly inhibited in the G3 (P=0.037) and G4 (P<0.001) groups (Fig. 6E).

Low-temperature plasma-activated solution shows improved safety in in vivo experiments. Liver and kidney function tests and routine blood tests were performed on the mice before the end of the experiment. As shown in Fig. 7, compared with the G1 control group, cisplatin caused a significant decrease in AST levels (0.01 ≤P<0.05*) and a significant increase in CREA levels (0.05 ≤P<0.01**), indicating that acute renal injury had occurred in the mice. However, no significant impairment of liver or kidney function was observed in the G2 or G3 group.

Fig. 8 shows the statistical analysis of routine blood test results in mice. Compared with those in the G1 control group, cisplatin treatment in the G4 group caused leukopenia (P=0.074), neutropenia (0.01 ≤P<0.05*) and thrombocytopenia (0.01 ≤P<0.05*). These results indicated that cisplatin caused bone marrow suppression in mice. In contrast, the G2 and G3 groups did not show any evidence of significant inhibition of hematopoietic function, although a slight increase in platelet count was observed in the G3 group (0.01 ≤P<0.05*).

Histological effects in tumor tissues. Hematoxylin/eosin staining and γ-H2AX and Ki-67 immunostaining were used to evaluate the histological effects in mouse tumors following treatment (Fig. 9). Hematoxylin/eosin staining revealed that tumor necrosis occurred in the G2-G4 groups. The PAS was injected into the tumors in the G2 and G3 groups. These tumors clearly showed great regional necrosis upon hematoxylin/eosin staining, whereas the chemotherapeutic drug cisplatin exhibited more uniform effects in the tumors. Similarly, in the tumor tissues of mice, γ-H2AX expression was observed in the G2-G4 groups, but the expression level in the G4 group was significantly greater than that in the other groups. In G2 and G3 groups, γ-H2AX was expressed around necrotic tumor tissues and displayed regional expression.

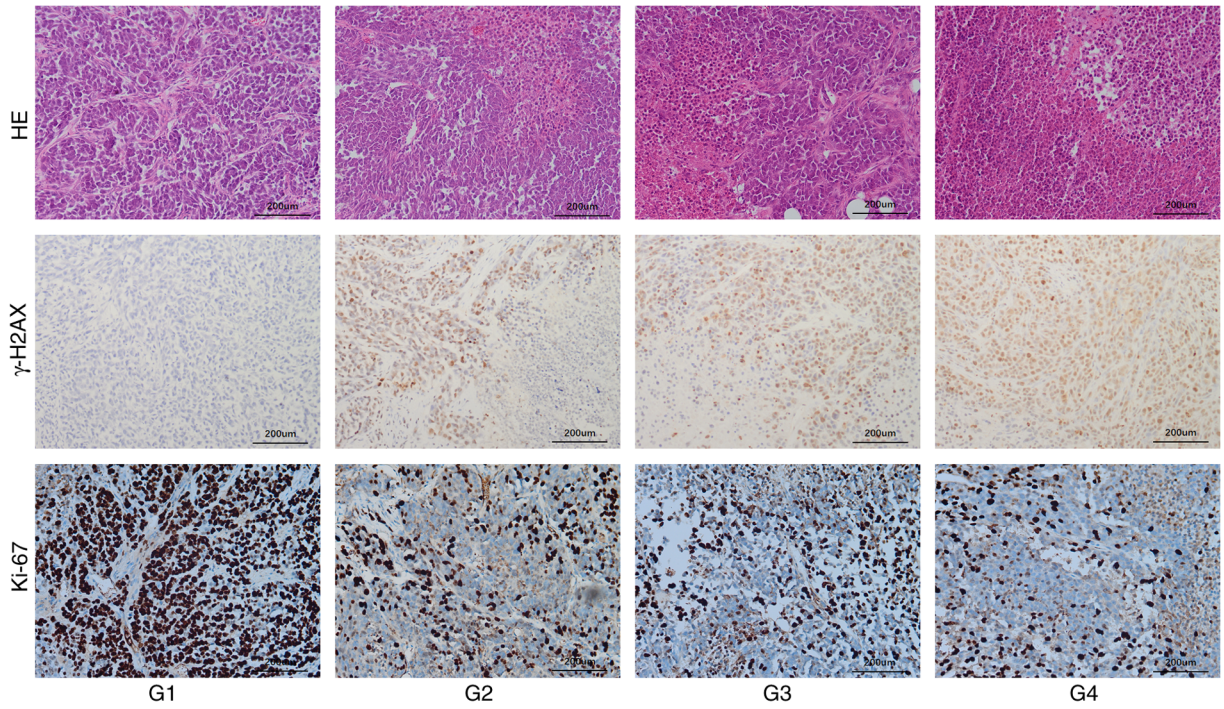

Figure 9. Hematoxylin/eosin staining was used to evaluate the histological effects of the tumor treatments on the mice. Immunohistochemical staining showed γ-H2AX and Ki-67 expression after tumor treatment in mice. HE, hematoxylin/eosin; H2AX, histone family 2A variant.

Ki-67 is a nuclear division- and proliferation-related protein and its function is closely related to mitosis; it is often used as a reliable marker of tumor cell proliferation. The greatest levels of tumor proliferation were noted in the control group. The percentage of Ki-67-positive cells was ~80% in control tumors, while the percentage of Ki-67-positive cells in the G2-G4 groups decreased to varying degrees.

Discussion

The present study described the antitumor effect of PAS on the melanoma cell line A375 cultured *in vitro* and subcutaneously transplanted tumors in mice. As a potential tumor treatment, low-temperature plasma therapy has been evaluated in a variety of tumor cell lines (5-7). However, most of the existing studies have focused on the direct effect of low-temperature plasma on cells cultured *in vitro*. Ongoing studies have shown that low-temperature plasma-activated DMEM has good antitumor effects (8,20,21). These results suggested that PAS also exhibits great potential in tumor treatment because the methodology eliminates the dependence on instruments and equipment in the treatment process. The effectiveness of direct treatment with low-temperature plasma may depend on the size and location of the tumor, as some deep solid tumors cannot be effectively treated (22,23). PAS can be injected deep into tumors (24,25), which overcomes the limitations of direct treatment and provides an accurate and effective method for tumor treatment.

The transfer of active substances from low-temperature plasma to a solution medium by physical or chemical means is the theoretical basis for the biological effects of PAS (26). It has been demonstrated that the active oxygen components and active nitrogen components in solution are the main active substances that induce biological effects, among which H_2O_2 is the most important (26,27). In our previous studies, changes in H_2O_2 and NO_3^- concentrations were also detected in DMEM and PBS exposed to a low-temperature plasma environment at different time points (28). The results showed that the concentrations of these active substances increased with increasing low-temperature plasma irradiation time (28). The results of the present study suggested that exposure to low-temperature plasma-activated PBS for a longer time will increase ROS levels in A375 cells. Catalase is an important antioxidant enzyme that plays important roles in scavenging ROS and maintaining the balance of the redox state (29). Under the same experimental conditions, catalase can significantly reduce the increase in intracellular ROS caused by treatment with PAS and further prevent cell death (5,30). These results also demonstrated that ROS in PAS are the main active components that cause cell damage.

Mitochondria are important organelle structures in cells and play leading roles in cell respiration and maintaining redox balance. They also play a central role in the apoptotic pathway (31,32). The present study showed that an increase in intracellular ROS levels leads to mitochondrial damage. When mitochondria are damaged, the permeability of the mitochondrial membrane increases and mitochondrial lipids are redistributed. The main feature of their structural change is mitochondrial swelling, which can be accompanied by a reduction or disappearance of the number of mitochondrial cristae. An increase in mitochondrial membrane permeability further leads to dysregulation of the distribution of protons and electrons in the inner membrane of the mitochondria and a decrease in or loss of the mitochondrial membrane potential. Maintenance of the mitochondrial membrane potential is necessary for mitochondrial respiratory function. Therefore, when

the mitochondrial membrane potential decreases, mitochondrial function is disrupted, which leads to apoptosis (33-35).

DNA damage and mitochondrial damage are the most common causes of damage to cancer cells treated with low-temperature plasma. Previous studies have shown that increases in intracellular ROS and DNA damage are observed after low-temperature plasma treatment (28,36,37). DNA double-strand breaks are the most important manifestation of damage. H2AX is a subtype of histone H2A. When DNA damage occurs in cells, H2AX is rapidly phosphorylated, producing γ-H2AX; therefore, γ-H2AX is a good marker of DNA damage (38). Using immunofluorescence technology, microscopic evaluation of γ-H2AX staining indicated regions of DNA double-strand breaks, with each focus corresponding to one DSB. When DNA damage cannot be repaired, cell cycle arrest occurs, leading to apoptosis.

At present, strategies for the treatment of cancer cells using low-temperature plasma are divided into direct and indirect treatments. Direct treatment involves direct irradiation of cancer cells or animal tumor models cultured *in vitro* with low-temperature plasma. Indirect treatment uses media activated by low-temperature plasma to further treat cancer cells *in vitro* or tumors *in vivo*. In existing studies, it has been confirmed that low-temperature plasma and PAS have clear anticancer effects on dozens of cancer cell lines cultured *in vitro*; however, for some non-superficial tumors, the use of direct treatment with low-temperature plasma is limited (5-7,9). Chen *et al* (2) developed a novel miniature CAP device (μCAP) that is directly connected to endoscopic devices and μCAP significantly inhibits the growth of brain gliomas in mice. Vaquero *et al* (39) established a mouse subcutaneous transplanted tumor model of cholangiocarcinoma and direct treatment of subcutaneous tumors with PAS yielded good antitumor effects. Notably, the jet of low-temperature plasma must contact the tumor to demonstrate effective antitumor effects. Therefore, for the treatment of solid tumors, local injection of PAS seems to represent a promising treatment strategy. Tanaka *et al* (40) used the cervical cell carcinoma line SiHa to establish a mouse subcutaneous transplantation tumor model and subcutaneously injected low-temperature plasma-activated Ringer's solution to treat the tumor, achieving good results. To demonstrate the safety of PAS, Nastasa *et al* provided mice with low-temperature plasma-activated water as a water source for 90 days. Low-temperature plasma-activated water did not cause functional damage or tissue damage to the heart, liver, kidney, brain, digestive system or blood system of mice (41). The present study, proposed a new treatment method. Specifically, PAS was injected into the tumor to allow the effective components in the solution to reach the tumor site more accurately. This treatment method can result in less toxicity and fewer side effects. When cisplatin was used to treat tumors, the mice experienced severe renal damage and bone marrow loss and were depressed and unable to eat. However, injection of the PAS into tumors did not significantly damage the liver, kidney or hematopoietic functions of the mice. Notably, hematoxylin and eosin and immunohistochemical staining of mouse tumor sections revealed that the tumors exhibited focal necrosis following injection of the PAS and that the DNA damage marker γ-H2AX was expressed around necrotic tissue. These phenomena indicated that the effective region of PAS is still limited even by intratumoral injection. Cisplatin, a chemotherapeutic drug, is transported to tumor sites through the blood circulation and can produce more extensive antitumor effects (42).

However, the present study had several limitations. First, only one fluid, namely, PBS, was used and no comparisons were made with different media. Second, although a number of researchers have conducted similar studies (5-7,8,28,37), the present study used only one cell line to validate the effect of PAS and errors due to chance could not be avoided. Finally, the present study used BALB mice for allogeneic implant modeling. This model lacks immune function and cannot reflect the immune microenvironment of the normal human body. In addition, several problems were exposed in this experiment. For example, the parameters and specifications of low-temperature plasma-forming devices have not yet been standardized and differences between *in vitro* and *in vivo* environments made it difficult to monitor the actual concentration of active substances. The authors are working on exploring more possibilities, such as using PAS to treat more melanoma cell lines of different origins as well as normal melanocytes to explore the specific mechanism of its killing effect on melanoma, using 3D tumor microenvironment models to explore the modulation of the tumor immune microenvironment by PAS and using mouse homologous melanoma cell implantation models to preserve the immune function of the mice in order to explore the PAS interacts with the immune microenvironment in an *in vivo* setting. In the future, it is hoped to develop a treatment method that combines PAS with novel materials to provide more durable, precise and uniform antitumor effects.

Low-temperature plasma has shown good antitumor effects in dozens of tumor cell lines. However, the method is limited by currently available instruments and equipment and is capable of only superficial penetration. PAS also showed good antitumor effects *in vitro*. The present study not only confirmed the effectiveness of local injection of PAS in the treatment of melanoma A375 cells and mice with tumors but also confirmed the safety of PAS in terms of hematopoietic, liver and kidney functions by monitoring the blood biochemistry of mice. Additional safety assessments need to be performed, such as an evaluation of the treatment's reproductive toxicity. In conclusion, the results of the present study confirmed that PAS represented a promising new agent for the treatment of melanoma.

Acknowledgements

The authors would like to thank Dr Ruru Wang and Dr Chen Bin (Anhui Province Key Laboratory of Environmental Toxicology and Pollution Control Technology, Hefei Institutes of Physical Science, Chinese Academy of Sciences, Anhui, China) for their help in experiments.

Funding

The present study was supported by the 2020 Natural Science Research Project of Anhui Universities, Anhui, China (Major Project), grant no. KJ2020ZD19 to Chunjun Yang, Clinical Cultivation Program of the Second Affiliated Hospital of Anhui Medical University, Anhui, China (Key

Project), grant no. 2020LCZD22 to Chunjun Yang, 2020 Provincial Quality Project of Colleges and University, grant no. 2020mooc227 and Spark Plan, Anhui Medical University, (grant no. 2015hhjh04).

Availability of data and materials

The data generated in the present study may be requested from the corresponding author.

Authors' contributions

The present study was conceived and designed by CY. The main experiments were conducted by XY and CChen. SZ and MR also conducted some experiments. As an expert in the field of cold atmospheric plasma, CCheng proposed the concept of the present study together with CY and participated in the drafting of the manuscript. CZ contributed to the experimental design of the present study and analyzed the experimental data. CY and CZ confirm the authenticity of all the raw data. All authors read and approved the final manuscript.

Ethics approval and consent to participate

The Anhui Medical University Laboratory Animal Ethics Committee (Anhui, China; approval no. LLSC20210406) approved the present study and approved experiments conducted at Jiangsu GemPharmatech Co., Ltd. (Jiangsu, China) as per the contract no. GJS04202101026

Patient consent for publication

Not applicable.

Competing interests

The authors declare that they have no competing interests.

References

1. Motaln H, Recek N and Rogelj B: Intracellular responses triggered by cold atmospheric plasma and plasma-activated media in cancer cells. Molecules 261: 336, 2021.
2. Chen Z, Simonyan H, Cheng X, Gjika E, Lin L, Canady J, Sherman JH, Young C and Keidar M: A novel micro cold atmospheric plasma device for glioblastoma both in vitro and in vivo. Cancers (Basel) 9: 61, 2017.
3. Arndt S, Unger P, Berneburg M, Bosserhoff AK and Karrer S: Cold atmospheric plasma (CAP) activates angiogenesis-related molecules in skin keratinocytes, fibroblasts and endothelial cells and improves wound angiogenesis in an autocrine and paracrine mode. J Dermatol Sci 89: 181-190, 2018.
4. Dubuc A, Monsarrat P, Virard F, Merbahi N, Sarrette JP, Laurencin-Dalicieux S and Cousty S: Use of cold-atmospheric plasma in oncology: A concise systematic review. Ther Adv Med Oncol 10: 433565781, 2018.
5. Aggelopoulos CA, Christodoulou AM, Tachliabouri M, Meropoulis S, Christopoulou ME, Karalis TT, Chatzopoulos A and Skandalis SS: Cold atmospheric plasma attenuates breast cancer cell growth through regulation of cell microenvironment effectors. Front Oncol 11: 826865, 2021.
6. Van Loenhout J, Flieswasser T, Freire Boullosa L, De Waele J, Van Audenaerde J, Marcq E, Jacobs J, Lin A, Lion E, Dewitte H, *et al*: Cold atmospheric plasma-treated pbs eliminates immunosuppressive pancreatic stellate cells and induces immunogenic cell death of pancreatic cancer cells. Cancers (Basel) 11: 1597, 2019.
7. Soni V, Adhikari M, Simonyan H, Lin L, Sherman JH, Young CN and Keidar M: In vitro and in vivo enhancement of temozolomide effect in human glioblastoma by non-invasive application of cold atmospheric plasma. Cancers (Basel) 13: 4485, 2021.
8. Zahedian S, Hekmat A, Tackallou SH and Ghoranneviss M: The impacts of prepared plasma-Activated medium (PAM) combined with doxorubicin on the viability of MCF-7 breast cancer cells: A new cancer treatment strategy. Rep Biochem Mol Biol 10: 640-652, 2022.
9. Yan D, Sherman JH and Keidar M: Cold atmospheric plasma, a novel promising anti-cancer treatment modality. Oncotarget 8: 15977-15995, 2017.
10. Yan D, Cui H, Zhu W, Nourmohammadi N, Milberg J, Zhang LG, Sherman JH and Keidar M: The specific vulnerabilities of cancer cells to the cold atmospheric plasma-stimulated solutions. Sci Rep 7: 4412-4479, 2017.
11. Privat-Maldonado A, Schmidt A, Lin A, Weltmann KD, Wende K, Bogaerts A and Bekeschus S: ROS from physical plasmas: Redox chemistry for biomedical therapy. Oxid Med Cell Longev 2019: 9062098, 2019.
12. Gan L, Zhang S, Poorun D, Liu D, Lu X, He M, Duan X and Chen H: Medical applications of nonthermal atmospheric pressure plasma in dermatology. J Dtsch Dermatol Ges 16: 7-13, 2018.
13. Long GV, Swetter SM, Menzies AM, Gershenwald JE and Scolyer RA: Cutaneous melanoma. Lancet 402: 485-502, 2023.
14. Leonardi GC, Falzone L, Salemi R, Zanghì A, Spandidos DA, Mccubrey JA, Candido S and Libra M: Cutaneous melanoma: From pathogenesis to therapy (Review). Int J Oncol 52: 1071-1080, 2018.
15. Strashilov S and Yordanov A: Aetiology and pathogenesis of cutaneous melanoma: Current concepts and advances. Int J Mol Sci 22: 6395, 2021.
16. Coelho SG and Hearing VJ: UVA tanning is involved in the increased incidence of skin cancers in fair-skinned young women. Pigment Cell Melanoma Res 23: 57-63, 2010.
17. Newton-Bishop J, Bishop DT and Harland M: Melanoma genomics. Acta Derm Venereol 100: adv138, 2020.
18. Rozeman EA, Dekker TJA, Haanen JBAG and Blank CU: Advanced melanoma: Current treatment options, biomarkers, and future perspectives. Am J Clin Dermatol 19: 303-317, 2018.
19. Zaib S, Hayyat A, Ali N, Gul A, Naveed M and Khan I: Role of mitochondrial membrane potential and lactate dehydrogenase a in apoptosis. Anticancer Agents Med Chem 22: 2048-2062, 2022.
20. Jo A, Bae JH, Yoon YJ, Chung TH, Lee EW, Kim YH, Joh HM and Chung JW: Plasma-activated medium induces ferroptosis by depleting FSP1 in human lung cancer cells. Cell Death Dis 13: 212, 2022.
21. Ikeda JI, Tanaka H, Ishikawa K, Sakakita H, Ikehara Y and Hori M: Plasma-activated medium (PAM) kills human cancer-initiating cells. Pathol In 68: 23-30, 2018.
22. Ishikawa K, Hosoi Y, Tanaka H, Jiang L, Toyokuni S, Nakamura K, Kajiyama H, Kikkawa F, Mizuno M and Hori M: Non-thermal plasma-activated lactate solution kills U251SP glioblastoma cells in an innate reductive manner with altered metabolism. Arch Biochem Biophys 688: 108414, 2020.
23. Griseti E, Merbahi N and Golzio M: Anti-cancer potential of two plasma-activated liquids: Implication of Long-lived reactive oxygen and nitrogen species. Cancers (Basel) 12: 721, 2020.
24. Fang T, Cao X, Shen B, Chen Z and Chen G: Injectable cold atmospheric plasma-activated immunotherapeutic hydrogel for enhanced cancer treatment. Biomaterials 300: 122189, 2023.
25. Solé-Martí X, Espona-Noguera A, Ginebra MP and Canal C: Plasma-conditioned liquids as anticancer therapies in vivo: Current state and future directions. Cancers (Basel) 13: 452, 2021.
26. Yan D, Talbot A, Nourmohammadi N, Cheng X, Canady J, Sherman J and Keidar M: Principles of using cold atmospheric plasma stimulated media for cancer treatment. Sci Rep 5: 18339, 2015.
27. Uchiyama H, Zhao QL, Hassan MA, Andocs G, Nojima N, Takeda K, Ishikawa K, Hori M and Kondo T: EPR-Spin trapping and flow cytometric studies of free radicals generated using cold atmospheric argon plasma and X-Ray irradiation in aqueous solutions and intracellular milieu. PLoS One 10: e136956, 2015.
28. Yang X, Yang C, Wang L, Cao Z, Wang Y, Cheng C, Zhao G and Zhao Y: Inhibition of basal cell carcinoma cells by cold atmospheric plasma-activated solution and differential gene expression analysis. Int J Oncol 56: 1262-1273, 2020.
29. Glorieux C and Calderon PB: Catalase, a remarkable enzyme: Targeting the oldest antioxidant enzyme to find a new cancer treatment approach. Biol Chem 398: 1095-1108, 2017.

30. Ahn HJ, Kim KI, Hoan NN, Kim CH, Moon E, Choi KS, Yang SS and Lee JS: Targeting cancer cells with reactive oxygen and nitrogen species generated by atmospheric-pressure air plasma. PLoS One 9: e86173, 2014.
31. Annesley SJ and Fisher PR: Mitochondria in health and disease. Cells 8: 680, 2019.
32. Dong L and Neuzil J: 'Chapter eight-mitochondria in cancer: Why mitochondria are a good target for cancer therapy' in Progress in Molecular Biology and Translational Science, Osiewacz HD, ed. (Academic Press), pp211-227, 2014.
33. Vafai SB and Mootha VK: Mitochondrial disorders as windows into an ancient organelle. Nature 491: 374-383, 2012.
34. Rickard BP, Overchuk M, Chappell VA, Kemal Ruhi M, Sinawang PD, Nguyen Hoang TT, Akin D, Demirci U, Franco W, Fenton SE, *et al*: Methods to evaluate changes in mitochondrial structure and function in cancer. Cancers (Basel) 15: 2564, 2023.
35. Wu S, Zhou F, Zhang Z and Xing D: Mitochondrial oxidative stress causes mitochondrial fragmentation via differential modulation of mitochondrial fission-fusion proteins. FEBS J 278: 941-954, 2011.
36. Wang L, Xia C, Guo Y, Yang C, Cheng C, Zhao J, Yang X and Cao Z: Bactericidal efficacy of cold atmospheric plasma treatment against multidrug-resistant Pseudomonas aeruginosa. Future Microbiol 15: 115-125, 2020.
37. Wang L, Yang X, Yang C, Gao J, Zhao Y, Cheng C, Zhao G and Liu S: The inhibition effect of cold atmospheric plasma-activated media in cutaneous squamous carcinoma cells. Future Oncol 15: 495-505, 2019.
38. Kuo LJ and Yang LX: Gamma-H2AX-a novel biomarker for DNA double-strand breaks. In Vivo 22: 305-309, 2008.
39. Vaquero J, Judée F, Vallette M, Decauchy H, Arbelaiz A, Aoudjehane L, Scatton O, Gonzalez-Sanchez E, Merabtene F, Augustin J, *et al*: Cold-atmospheric plasma induces tumor cell death in preclinical in vivo and in vitro models of human cholangiocarcinoma. Cancers (Basel) 12: 1280, 2020.
40. Tanaka H, Nakamura K, Mizuno M, Ishikawa K, Takeda K, Kajiyama H, Utsumi F, Kikkawa F and Hori M: Non-thermal atmospheric pressure plasma activates lactate in Ringer's solution for anti-tumor effects. Sci Rep 6: 36282, 2016.
41. Nastasa V, Pasca AS, Malancus RN, Bostanaru AC, Ailincai LI, Ursu EL, Vasiliu AL, Minea B, Hnatiuc E and Mares M: Toxicity assessment of long-term exposure to non-thermal plasma activated water in mice. Int J Mol Sci 22: 11534, 2021.
42. Dasari S and Tchounwou PB: Cisplatin in cancer therapy: Molecular mechanisms of action. Eur J Pharmacol 740: 364-378, 2014.